

Multi-branch successive interference cancellation for MIMO spatial multiplexing systems: design, analysis and adaptive implementation

R. Fa R.C. de Lamare

Communications Research Group, Department of Electronics, University of York, YO10 5DD, UK
 E-mail: r.fa@liverpool.ac.uk

Abstract: In this study, the authors propose a novel successive interference cancellation (SIC) strategy for multiple-input multiple-output spatial multiplexing systems based on a structure with multiple interference cancellation branches. The proposed multi-branch SIC (MB-SIC) structure employs multiple SIC schemes in parallel and each branch detects the signal according to its respective ordering pattern. By selecting the branch which yields the estimates with the best performance according to the selection rule, the MB-SIC detector, therefore, achieves higher detection diversity. The authors consider three selection rules for the proposed detector, namely, the maximum likelihood (ML), the minimum mean square error and the constant modulus criteria. An efficient adaptive receiver is developed to update the filter weight vectors and estimate the channel using the recursive least squares algorithm. Furthermore a bit error probability performance analysis is carried out. The simulation results reveal that the authors' scheme successfully mitigates the error propagation and approaches the performance of the optimal ML detector, while requiring a significantly lower complexity than the ML and sphere decoder detectors.

1 Introduction

The deployment of multiple transmit and receive antennas has been recognised to improve wireless link performance in communication system significantly. The degrees of freedom, which are afforded by the multiple antennas, can offer dramatic multiplexing [1–5] and diversity gains [6, 7]. The diversity gains make the links more reliable and allow low error rates over wireless fading channels, whereas the multiplexing gains enable high spectral efficiencies. Within the scope of this paper, we focus on the multiplexing gains obtained by the multiple-input multiple-output (MIMO) system.

In a spatial multiplexing configuration, in order to separate all data streams using their respective spatial signatures, the designer may resort to several detection techniques, which are similar to multiuser detection methods [8]. The optimal maximum likelihood (ML) performance can be approached using the sphere decoding algorithm [9, 10]. However, the complexity of this algorithm can be polynomial or exponential depending on the signal-to-noise ratio (SNR) and the signal constellation, typically very high for low to moderate SNR values. As known to all, it is typical for coded systems that detectors normally operate at low to moderate SNR values. This renders the application of the sphere decoder (SD) limited and has motivated the development of various alternative low-complexity strategies.

The diagonal Bell Laboratories Layered Space-Time (D-BLAST) proposed by Foschini [3] was the first BLAST

architecture. Owing to the large computational complexity required for the D-BLAST scheme, a simplified version, called the vertical BLAST (V-BLAST) has been proposed in [4, 5]. The V-BLAST scheme is primarily based on the following three steps: (i) ordering to select the substream with the largest SNR; (ii) interference nulling by using the zero forcing or the minimum mean-square-error (MMSE) criterion to reduce the effect of interfering signals on the desired one and (iii) successive interference cancellation (SIC) [11]. According to this view, the V-BLAST can be seen as an ordered SIC. There is also a number of other strategies to achieve the capacity gain of MIMO systems including the linear and the decision feedback (DF) detector [12–15] and the parallel interference cancellation (PIC) [16, 17]. However, all these detectors suffer from performance degradation. It motivates us to develop an effective detector with an affordable complexity.

In this paper, we propose a novel SIC strategy for MIMO spatial multiplexing systems based on multiple processing branches. This multi-branch SIC (MB-SIC) framework consists of several SIC branches placed in parallel and in each branch an SIC scheme detects the signal with a given ordering pattern. From this point of view, the SIC branch with the optimal ordering pattern, which detects the signal according to the signal-to-interference-plus-noise ratio (SINR) from high to low, is tantamount to the ordered SIC scheme used in the V-BLAST detector. Using the designed selection rule, which determines the branch with the best performance, the detection diversity is obtained by

exploiting different detection ordering patterns. Thus, the full detection diversity in this case can be achieved by permuting all possible ordering patterns. Based on different application requirements, different criteria, such as ML, MMSE and constant modulus (CM), can be used as selection rules to select the branch with the best performance. Owing to the high computational complexity of the optimal ordering scheme, we propose three sub-optimum ordering schemes for practical implementation, which select subsets of ordering patterns from the optimal ordering scheme set. In an attempt to reduce the computational complexity of our proposed algorithm, an efficient adaptive receiver is developed to update the filter weight vectors and estimate the channel using the recursive least squares (RLS) algorithm. An adaptive equalisation of flat-fading MIMO channels has been proposed in [18] by taking advantage of the equivalence between the V-BLAST receiver and the generalised decision feedback equaliser (GDFE) [19]. The adaptive architecture in [18] is adopted to implement the SIC detector for each branch so that a great deal of computation can be saved. Furthermore, a bit error probability (BEP) performance analysis is carried out. The simulation and analytical results reveal that our scheme successfully mitigates error propagation and approaches the performance of the optimal ML detector.

The main contributions we have made in our paper are as follows:

1. A novel MB-SIC strategy for MIMO spatial multiplexing systems is proposed. Three selection rules, together with the proposed scheme, are investigated.
2. Three sub-optimum ordering schemes are proposed to reduce the computational complexity.
3. An efficient adaptive implementation using the RLS algorithm is developed for the proposed receiver.
4. A BEP analysis is carried out for both the V-BLAST and the proposed receiver.

This paper is organised as follows. Section 2 briefly describes a MIMO spatial multiplexing system model and reviews some existing detectors. Section 3 is dedicated to the presentation of the novel MB-SIC detector. The adaptive implementation of the proposed scheme and its computational complexity are presented in Section 4. In Section 5, the BEP performance analysis is carried out. Section 6 presents and discusses the numerical simulation results, while Section 7 gives the conclusions.

2 System model

In this section, to start with, we briefly describe a MIMO spatial multiplexing system model. Subsequently, some existing detection schemes including ML, the SD, the linear detector and the V-BLAST, are reviewed. Owing to either the high computational complexity or the unacceptable performance, these schemes are prohibitive for practical use.

2.1 Transmitter

Let us consider a spatial multiplexing MIMO system, as depicted in Fig. 1a, with N_T transmit antennas and N_R receive antennas, where $N_R \geq N_T$. At each time instant $[i]$, the system transmits N_T symbols which are organised into an $N_T \times 1$ vector $\mathbf{s}[i] = [s_1[i], s_2[i], \dots, s_{N_T}[i]]^T$ taken from a modulation constellation $A = \{a_1, a_2, \dots, a_N\}$, where

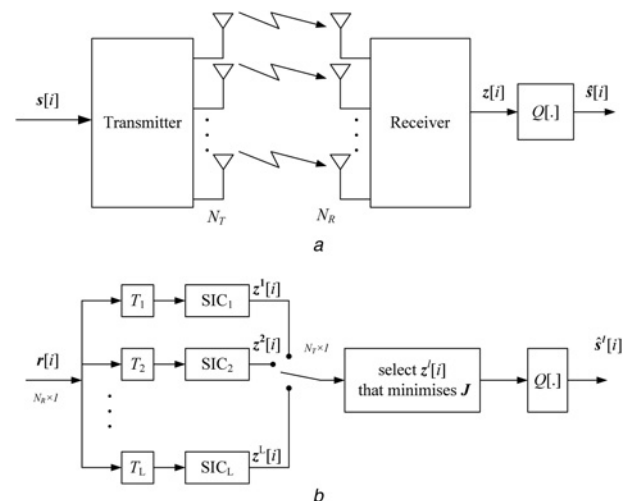


Fig. 1 Overview diagram for the proposed system

a MIMO spatial multiplexing system

b Global block diagram of the proposed MB-SIC detector

$(\cdot)^T$ denotes transpose. The symbol vector $\mathbf{s}[i]$ is then transmitted over flat fading channels and the signals are demodulated and sampled at the receiver, which is equipped with N_R antennas. The received signal is collected into an $N_R \times 1$ vector $\mathbf{r}[i] = [r_1[i], r_2[i], \dots, r_{N_R}[i]]^T$ given by

$$\mathbf{r}[i] = \mathbf{H}\mathbf{s}[i] + \mathbf{v}[i] \quad (1)$$

where the $N_R \times 1$ vector $\mathbf{v}[i]$ is a zero mean complex circular symmetric Gaussian noise with covariance matrix $E[\mathbf{v}[i]\mathbf{v}^H[i]] = \sigma_v^2 \mathbf{I}$, where $E[\cdot]$ stands for the expected value, $(\cdot)^H$ denotes the Hermitian operator, σ_v^2 is the noise variance and \mathbf{I} is the identity matrix. The symbol vector $\mathbf{s}[i]$ has zero mean and a covariance matrix $E[\mathbf{s}[i]\mathbf{s}^H[i]] = \sigma_s^2 \mathbf{I}$, where σ_s^2 is the signal power. The elements h_{n_R, n_T} of the $N_R \times N_T$ channel matrix \mathbf{H} correspond to the complex channel response from the n_T th transmit antenna to the n_R th receive antenna.

2.2 Conventional detection techniques for spatial multiplexing

The optimal detection algorithm is the ML detection algorithm given by

$$\hat{\mathbf{s}}_{ML}[i] = \arg \min_{\hat{\mathbf{s}} \in A} \|\mathbf{r}[i] - \mathbf{H}\hat{\mathbf{s}}[i]\|^2 \quad (2)$$

where A denotes a set of N_T -dimensional candidate vectors. The computational complexity, which increases exponentially with the number of transmit antennas, prevents the practical application of the ML detector. The SD is a powerful scheme to approach the ML detection solution of signals observed at the output of MIMO systems. However, the complexity of this algorithm can be polynomial or exponential depending on the noise variance and the signal constellation [9, 10]. This has motivated the development of various suboptimal detection techniques. The MMSE linear detector is a relatively simple strategy to separate the transmitted signals at the receiver. It corresponds to designing an $N_R \times N_T$ parameter matrix \mathbf{W} according to the MMSE criterion. The design of the MMSE filter matrix \mathbf{W} is based on the optimisation of the following

cost function

$$J(\mathbf{W}) = E[\|\mathbf{s}[i] - \mathbf{W}^H \mathbf{r}[i]\|^2] \quad (3)$$

By computing the gradient of (3) with respect to \mathbf{W} and then making it equal to a null matrix, we obtain the $N_R \times N_T$ MMSE filter matrix

$$\mathbf{W} = \left(\mathbf{H}\mathbf{H}^H + \frac{\sigma_v^2}{\sigma_s^2} \mathbf{I} \right)^{-1} \mathbf{H} \quad (4)$$

The MMSE linear detector expression above requires the channel matrix \mathbf{H} (in practice an estimate of it) and the noise variance σ_v^2 at the receiver. There are a number of other strategies to achieve the capacity gain of MIMO systems in which the V-BLAST is the most competitive one because of its lower complexity and good performance. The linear and the DF detectors [12–15] and the PIC [16, 17], also provide alternatives to avoiding high computational complexity. However, there is still a large performance gap between these algorithms and the ML-type detectors.

3 Multi-branch SIC detection

This section is devoted to the description of the proposed MB-SIC detector for MIMO systems. We present the overall principles and structures of the proposed scheme in the first place, and then we introduce the selection rules and ordering schemes that are employed in our proposed detector subsequently. Based on different application requirements and system structures, better performance and lower complexity can be achieved by employing a proper selection rule and ordering scheme.

3.1 Proposed scheme

The proposed detection structure employs SICs on several parallel branches that are equipped with different ordering patterns. Namely, each branch produces a symbol estimate vector by exploiting a certain ordering pattern. Thus, there is a group of symbol estimate vectors at the end of the MB structure. We present MMSE-SIC for the design of the proposed MB MIMO receiver because the MMSE estimator usually has good performance, is mathematically tractable and has relatively simple adaptive implementation. The novel structure for detection exploits different patterns and orderings for the modification of the original V-BLAST architecture and achieves higher detection diversity by selecting the branch which yields the estimates with the best performance.

Fig. 1b depicts the global block diagram of the proposed detector. In order to detect the transmitted signals using the proposed MB-SIC structure, the detection process for each branch uses linear MMSE nulling and symbol successive cancellation to compute $\tilde{\mathbf{z}}_l[i] = [\tilde{z}_{l,1}[i], \tilde{z}_{l,2}[i], \dots, \tilde{z}_{l,N_T}[i]]^T$, where $\tilde{\mathbf{z}}_l[i]$ denotes the $N_T \times 1$ ordered symbol estimate vector for the l th branch. Let $\tilde{\mathbf{s}}_l[i] = \mathbf{T}_l \mathbf{s}[i] = [\tilde{s}_{l,1}[i], \tilde{s}_{l,2}[i], \dots, \tilde{s}_{l,N_T}[i]]^T$ denote the ordered set, which is a permutation of the transmitted symbol set $\mathbf{s}[i]$ ordered by the transformation matrix \mathbf{T}_l , $l = 1, \dots, L$. The transformation matrices \mathbf{T}_l , $l = 1, \dots, L$, in which each row and each column contain only one 1, corresponds to the ordering pattern employed in the l th branch. It is worth noting that $\tilde{z}_l[i]$ is detected according to the order

determined by \mathbf{T}_l . Thus, to select the best estimate vector conveniently, we simply transform $\tilde{\mathbf{z}}_l[i]$ to $\mathbf{z}_l[i]$ by using \mathbf{T}_l as

$$\mathbf{z}_l[i] = \mathbf{T}_l^T \tilde{\mathbf{z}}_l[i] \quad (5)$$

The non-adaptive implementation of the l -th SIC branch, as shown in Fig. 2a, is mathematically given as follows

$$\tilde{\mathbf{z}}_{l,n}[i] = \mathbf{W}_{l,n}^H[i] \mathbf{r}_{l,n}[i] \quad (6)$$

where

$$\begin{aligned} \mathbf{r}_{l,n}[i] &= \mathbf{r}[i], \quad n = 1 \\ \mathbf{H}' &= \mathbf{T}_l \mathbf{H} \\ \mathbf{r}_{l,n}[i] &= \mathbf{r}[i] - \sum_{k=1}^{n-1} (\mathbf{H}')_k \tilde{s}_{l,k}[i], \quad n \geq 2 \\ \mathbf{W}_{l,n} &= \left(\bar{\mathbf{H}}_n' \bar{\mathbf{H}}_n'^H + \frac{\sigma_v^2}{\sigma_s^2} \mathbf{I} \right)^{-1} (\mathbf{H}')_n \\ \tilde{s}_{l,n}[i] &= Q(\tilde{z}_{l,n}[i]) \end{aligned} \quad (7)$$

where $(\mathbf{H}')_n$ denotes the n th column of \mathbf{H}' , $\bar{\mathbf{H}}_n'$ denotes the matrix obtained by taking columns $n, n + 1, \dots, N_T$ of \mathbf{H}' and $Q(\cdot)$ is the quantisation function. In summary, the basic principle of the proposed structure is to modify the ordering of the original ordered SIC in appropriate ways such that the detector can obtain a group of different estimate vectors and then select the most likely symbol estimates based on a certain selection rule, which will be introduced in the following section. The simulation results reveal that our scheme successfully mitigates the error propagation and approaches the performance of the optimal ML detector.

3.2 Selection rules

The proposed MB-SIC detector selects the branch that optimises the corresponding cost function J according to

$$l_{\text{opt}} = \arg \min_{1 \leq l \leq L} J(l) \quad (8)$$

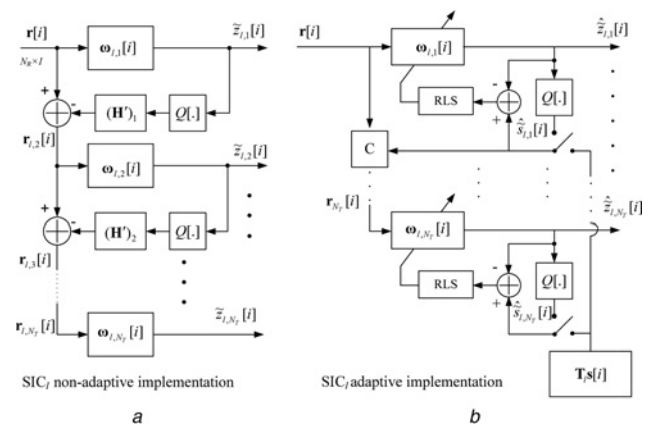


Fig. 2 Schematic structures of the l th SIC branch

a Schematic structure of the l th SIC branch with non-adaptive implementation
 b Schematic structure of the l th SIC branch with adaptive implementation

The final detected symbol is

$$\hat{s}_r[i] = Q(z_{r,\text{opt}}[i]) \quad (9)$$

Based on different application requirements, different criteria, such as the ML, the MMSE and the CM, can be used as selection rules to select the branch with the best performance.

3.2.1 ML (or minimum Euclidean distance) criterion:

The cost function for the ML criterion, which is equivalent to the minimum Euclidean distance criterion, is written as

$$J_{\text{ML}}(l) = \|r[l] - H\hat{s}_l[l]\|^2 \quad (10)$$

The ML criterion can provide the best performance among these candidate criteria while channel information is available. Although the channel estimation would cost extra complexity, the performance improvement by employing the ML criterion is considerable.

3.2.2 MMSE criterion:

Where channel information is not available, the MMSE criterion can be used to select the branch which minimises the mean square error of transmitted symbols. The cost function is given by

$$J_{\text{MMSE}}(l) = \|\hat{s}_l[l] - z_l[l]\|^2 \quad (11)$$

where $\hat{s}[i]$ is symbol estimation in the decision directed mode; thus, the MMSE criterion would be greatly impaired by error propagation.

3.2.3 Constant modulus criterion: The CM algorithm originally proposed by Godard [20] has widely been applied to the blind detection because of its robustness and easy implementation. In this context, the CM criterion attempts to minimise the cost function

$$J_{\text{CM}}(l) = \sum_{n=1}^{N_T} [||z_{l,n}[i]|^2 - 1|^2] \quad (12)$$

We will show how these selection rules perform later in the simulation section. Note that for non-constant modulus constellations such as QAM, one can replace the cost function in (12) with a square contour [21].

3.3 Ordering schemes

Here, we propose the optimal ordering scheme and three alternative ordering schemes for designing the proposed receiver, where the common framework is the use of parallel branches with ordering patterns that yield a group of symbol estimate vectors. The number of parallel branches L is a parameter that must be chosen by the designer. In this context, the optimal ordering scheme conducts an exhaustive search $L = N_T!$ where $!$ is the factorial operator. Taking a 4×4 system for example, Fig. 3 shows all ordering patterns that can be employed in the SIC detector. There are 24 ordering patterns in the optimal ordering scheme. It is clearly very complex for practical systems, especially when N_T is large. Therefore an ordering scheme with low complexity, which renders itself to practical implementation, is of great interest.

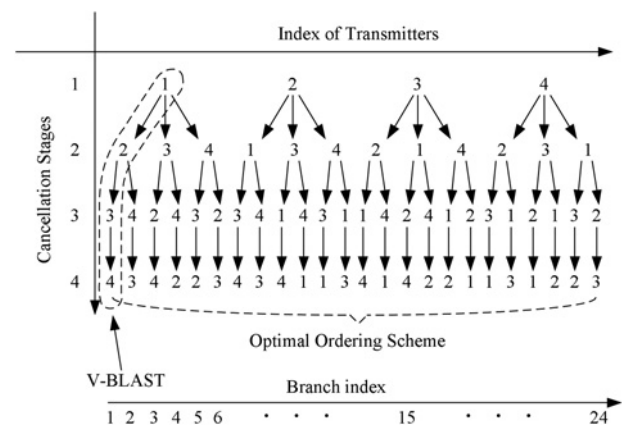


Fig. 3 Illustration of the ordering scheme for a 4×4 system

To this end, we propose three sub-optimal schemes to design the transformation matrices T_l with appropriate structures such that they can be used for low-complexity implementation of the detector. These three schemes are developed to select a subset from the optimal ordering scheme set in a smart way. We assume that the original order has been sorted according to optimal order (maximum SINR criterion), that is, as illustrated in Fig. 3, the V-BLAST order is the first order (index 1) in the the optimal ordering scheme set. This optimal ordering scheme set can be easily obtained by using `PERMS($N_T : -1 : 1$)` in Matlab.

3.3.1 Pre-stored patterns (PSP): The transformation matrix T_1 for the first branch is chosen as the identity matrix I_{N_T} to keep the optimal ordering as described by $T_1 = I_{N_T}$. The remaining ordering patterns can be described mathematically by

$$T_l = \begin{bmatrix} I_s & \mathbf{0}_{s, N_T-s} \\ \mathbf{0}_{N_T-s, s} & \phi[I_{N_T-s}] \end{bmatrix}, 2 \leq l \leq N_T \quad (13)$$

where $\mathbf{0}_{m,n}$ denotes an $m \times n$ -dimensional matrix full of zeros, the operator $\phi[\cdot]$ rotates the elements of the argument matrix column-wise such that an identity matrix becomes a matrix with ones in the reverse diagonal. The proposed ordering algorithm shifts the ordering of the cancellation according to shifts given by

$$s = (l - 2), 2 \leq l \leq N_T \quad (14)$$

Note that in this scheme, the number of branches is equal to the number of transmitter antennas.

3.3.2 Frequently selected branches (FSB): The basic principle of the proposed FSB algorithm is to build a codebook that contains the ordering patterns for the most likely selected branches. In order to build such codebook, we resort to a simulation approach, where we identify the statistics of each selected branch and construct the codebook with the L most likely selected branches to be encountered. The algorithm is summarised in Fig. 4, where d_E denotes the vector of Euclidean distance for all possible branches, N_e denotes the total number of experiments we did, L_{idv} is defined for the storage of the selected branches for every experiment and L_o is the codebook for optimal ordering patterns computed by `PERMS($N_T : -1 : 1$)`, which provides the list containing all possible permutations

```

1:  $\mathbf{d}_E \leftarrow \text{NULL}, \mathbf{L}_{idx} \leftarrow \text{NULL}, \mathbf{L}_{FSB} \leftarrow \text{NULL}$ 
2:  $L_{opt} \leftarrow N_T!, l \leftarrow 1$ 
3:  $\mathbf{L}_o \leftarrow \text{PERMS}(N_T : -1 : 1)$ 
4: for  $n_e = 1$  to  $N_e$  do
5:   for  $l = 1$  to  $L_{opt}$  do
6:      $\mathbf{T}_l \leftarrow \mathbf{L}_o(l)$ 
7:      $\hat{\mathbf{s}}_l[i] \leftarrow \text{SIC}(\mathbf{T}_l \mathbf{H})$ 
8:      $\mathbf{d}_E[l] \leftarrow \|\mathbf{r}[i] - \mathbf{H}\hat{\mathbf{s}}_l[i]\|$ 
9:   end for
10:   $\mathbf{L}_{idx}(n_e) \leftarrow \text{MIN\_Index}(\mathbf{d}_E)$ 
11: end for
12:  $\mathbf{L}_{FSB} \leftarrow \text{SELECT}(\text{HIST}(\mathbf{L}_{idx}), L)$ 

```

Fig. 4 FSB ordering scheme

of the N_T elements. We highlight that in each run, after we measure the Euclidean distances for all branches, the branch that brings the minimum Euclidean distance is stored in \mathbf{L}_{idx} at step 10. Finally, the FSB codebook \mathbf{L}_{FSB} is created by selecting the most frequently selected L branches according to the histogram of \mathbf{L}_{idx} . The selected ordering patterns and their probabilities of being selected are shown in Table 1. An interesting fact is that the FSB codebooks with ten elements for 4×4 , 6×6 and 8×8 systems are almost same and the probabilities of selecting these ordering patterns for 4×4 , 6×6 and 8×8 systems are all more than 99%. We note that rankings for these ordering patterns are slightly different for different systems. The possible reason for this might be that the number of experiments N_e is not sufficiently large. However, we believe that the ranking would not affect the system performance significantly.

3.3.3 Listing patterns approach (LPA): Motivated by the fact that we have to do a lot of prior work before the FSB algorithm can be employed, we propose an online codebook updating algorithm, which is called LPA. However, this approach is restricted by the number of antennas. We suppose that the channel is block-fading in which a block of symbols are affected by the same fading value. Thus, once the channel changes, we would re-select a list of ordering patterns to update the codebook. In this case, the LPA algorithm is proposed to fulfil the online updating of the codebook. We formalise the algorithm in Fig. 5. In each block which is supposed to contain L_b frames, we use the optimal ordering scheme that

```

1:  $\mathbf{d}_E \leftarrow \text{NULL}, \mathbf{L}_{LPA} \leftarrow \text{NULL}$ 
2:  $L_{opt} \leftarrow N_T!, l \leftarrow 1$ 
3:  $\mathbf{L}_o \leftarrow \text{PERMS}(N_T : -1 : 1)$ 
4: for  $i = 1$  to  $L_b$  do
5:   if  $i == 1$  then
6:     for  $l = 1$  to  $L_{opt}$  do
7:        $\mathbf{T}_l \leftarrow \mathbf{L}_o(l)$ 
8:        $\hat{\mathbf{s}}_l[i] \leftarrow \text{SIC}(\mathbf{T}_l \mathbf{H})$ 
9:        $\mathbf{d}_E[l] \leftarrow \|\mathbf{r}[i] - \mathbf{H}\hat{\mathbf{s}}_l[i]\|$ 
10:    end for
11:     $\mathbf{L}_{LPA} \leftarrow \text{SELECT}(\mathbf{d}_E, L)$ 
12:   else
13:     for  $l = 1$  to  $L$  do
14:        $\mathbf{T}_l \leftarrow \mathbf{L}_{LPA}(l)$ 
15:        $\hat{\mathbf{s}}_l[i] \leftarrow \text{SIC}(\mathbf{T}_l \mathbf{H})$ 
16:        $\mathbf{d}_E[l] \leftarrow \|\mathbf{r}[i] - \mathbf{H}\hat{\mathbf{s}}_l[i]\|$ 
17:     end for
18:   end if
19: end for

```

Fig. 5 LPA ordering scheme

exhaustively searches all possible orderings in the first frame, then updates the codebook \mathbf{L}_{LPA} online by listing the first L ordering patterns that minimise the cost function. Thereafter, we detect the remaining frames by using the updated codebook \mathbf{L}_{LPA} .

4 Adaptive implementation

The proposed MB-SIC detector shown in the previous section not only requires the channel matrix \mathbf{H} and the noise variance σ_n^2 at receiver, but also requires the inversion of an $N_R \times N_R$ matrix and other operations, whose complexity is $\mathcal{O}(N_R^3)$. To reduce the complexity of our proposed detector and to allow it to operate in time-varying scenarios, we develop an adaptive implementation for the receiver filters and a channel estimator based on the RLS algorithm.

4.1 RLS algorithm

An adaptive equalisation of flat-fading MIMO channels has been proposed in [18] by taking advantage of the equivalence between the V-BLAST receiver and the GDFE [19]. The algorithm is the adaptive V-BLAST structure in

Table 1 Selected patterns and their probabilities of being selected by FSB ordering scheme (ranked)

Index	4 × 4 system	Index	6 × 6 system	Index	8 × 8 system
1	0.9971	1	0.9514	1	0.9388
2	1.935×10^{-3}	2	1.446×10^{-2}	2	1.542×10^{-2}
5	4.943×10^{-4}	5	8.217×10^{-3}	3	7.684×10^{-3}
3	1.813×10^{-4}	3	5.324×10^{-3}	5	5.311×10^{-3}
19	1.285×10^{-4}	17	4.03×10^{-3}	4	5.254×10^{-3}
17	6×10^{-5}	13	2.233×10^{-3}	13	3.164×10^{-3}
13	3.6×10^{-5}	19	2.22×10^{-3}	17	2.542×10^{-3}
4	1.4×10^{-5}	4	1.529×10^{-3}	21	1.977×10^{-3}
6	1.1×10^{-5}	21	1.291×10^{-3}	19	1.582×10^{-3}
21	1×10^{-5}	6	1.284×10^{-3}	6	1.073×10^{-3}
⋮	⋮	25	7.8×10^{-4}	49	6.073×10^{-4}
⋮	⋮	⋮	⋮	⋮	⋮

which both the taps and the detection ordering are updated recursively in time. In this section, we introduce the adaptive implementation, which only updates the taps, into our design. The adaptive SICs using the RLS algorithm are employed in the branches of the proposed receiver. Fig. 2b depicts the adaptive implementation of the l th SIC branch, which works in two modes. The first mode is a training mode and the second is a decision-directed mode. The filters are trained by using training sequence $s[i]$, which is known to the receiver. The detection is started with linear filtering for the first substream, and the determined symbol is fed back and is concatenated together with the original input vector. The transmitted symbols in $s[i]$ are detected successively, and, the degree of the linear filter increases with the number of detected symbols. To be specific, the following notations are introduced: $\mathbf{W}_{l,n}[i]$ denotes $(N_R + n - 1)$ -dimensional weight vectors at the l th branch; $\mathbf{r}_n[i]$ denotes the input vector to the n th linear filter; and $\hat{z}_{l,n}[i]$ denotes the n th linear filter output, where $n \in \{1, 2, \dots, N_T\}$; $\mathbf{T}_l s[i]$ denotes the training sequence for the l th branch and the order of detection is determined by the ordering pattern \mathbf{T}_l . Note that in the training mode, $\hat{s}_{l,n}[i] \in \mathbf{T}_l s[i]$ represents the training symbol, while in the decision-directed mode, $\hat{s}_{l,n}[i]$ is substituted by the detected symbol $Q(\hat{z}_{l,n}[i])$. The output of the linear filter can be represented as

$$\hat{z}_{l,n}[i] = \mathbf{W}_{l,n}^H[i] \mathbf{r}_{l,n}[i] \quad (15)$$

where

$$\begin{aligned} \mathbf{r}_{l,n}[i] &= \mathbf{r}[i], & n &= 1 \\ \mathbf{r}_{l,n}[i] &= [\mathbf{r}_{l,n-1}^T[i], \hat{s}_{l,n}[i]]^T, & n &= 2, \dots, N_T \end{aligned} \quad (16)$$

The weight vectors $\mathbf{W}_{l,n}[i]$ in (15) can be obtained by solving the standard least squares (LS) problem. Specifically, the LS cost function with an exponential window is given by

$$\mathcal{J}_n[i] = \sum_{k=1}^i \lambda^{i-k} |\hat{z}_{l,n}[i] - \mathbf{W}_{l,n}^H[i] \mathbf{r}_{l,n}[i]|^2 \quad (17)$$

The optimal tap weight minimising $\mathcal{J}_n[i]$ is given by

$$\mathbf{W}_{l,n}[i] = \mathbf{R}_{l,n}^{-1}[i] \mathbf{p}_{l,n}[i] \quad (18)$$

where $\mathbf{R}_{l,n}[i]$ is the time-averaged correlation matrix defined by

$$\mathbf{R}_{l,n}[i] = \sum_{k=1}^i \lambda^{i-k} \mathbf{r}_{l,n}[k] \mathbf{r}_{l,n}^H[k] \quad (19)$$

and $\mathbf{p}_{l,n}[i]$ is the time-averaged cross correlation vector defined by

$$\mathbf{p}_{l,n}[i] = \sum_{k=1}^i \lambda^{i-k} \mathbf{r}_{l,n}[k] \hat{s}_{l,n}[k] \quad (20)$$

It is well known that the optimal weight in (18) can be calculated recursively using the RLS algorithm, which is

summarised as follows

$$\begin{aligned} \Phi_{l,n}[0] &= \delta^{-1} \mathbf{I} \\ \mathbf{k}_{l,n}[i] &= \frac{\lambda^{-1} \Phi_{l,n}[i] \mathbf{r}_{l,n}[i]}{1 + \lambda^{-1} \mathbf{r}_{l,n}^H[i] \Phi_{l,n}[i] \mathbf{r}_{l,n}[i]} \\ \Phi_{l,n}[i] &= \lambda^{-1} \Phi_{l,n}[i-1] - \lambda^{-1} \mathbf{k}_{l,n}[i] \mathbf{r}_{l,n}^H[i] \Phi_{l,n}[i] \\ \mathbf{W}_{l,n}[i] &= \mathbf{W}_{l,n}[i-1] + \mathbf{k}_{l,n}[i] \xi_{l,n}^*[i] \end{aligned} \quad (21)$$

where δ is a small constant, $\mathbf{k}_{l,n}[i]$ is the gain vector for the l th branch, and $\xi_{l,n}[i]$ is the estimation error defined by

$$\xi_{l,n}[i] = \hat{s}_{l,n}[i] - \mathbf{W}_{l,n}^H[i] \mathbf{r}_{l,n}[i] \quad (22)$$

and $(\cdot)^*$ denotes conjugate operator.

4.2 Channel estimation

In this paper, we employ the LS MIMO channel estimation algorithm which has been investigated in [22]. In the LS algorithm, the interested channel estimation must minimise the cost function whose expression at the time instant i is defined based on a weighted average of error squares as

$$\mathcal{J}[i] = \sum_{k=1}^i \lambda^{i-k} \|\mathbf{r}[k] - \hat{\mathbf{H}}[i] \mathbf{s}[k]\|^2 \quad (23)$$

where $\mathbf{r}[k]$ and $\mathbf{s}[k]$ are the received and transmitted symbol vectors at the time instant k , respectively, λ is the forgetting factor and $\hat{\mathbf{H}}[i]$ is the channel matrix estimate at the time instant i .

To minimise the cost function, the gradient of the cost function with regard to channel matrix estimate must be set to the zero matrix as

$$\begin{aligned} -\frac{1}{2} \nabla_{\hat{\mathbf{H}}[i]} \mathcal{J}[i] &= \sum_{k=1}^i \lambda^{i-k} [\mathbf{r}[k] - \hat{\mathbf{H}}[i] \mathbf{s}[k]] \mathbf{s}[k]^H \\ &= \mathbf{0}_{N_R, N_T} \end{aligned} \quad (24)$$

By solving (24), we obtain the LS estimate of the channel matrix as

$$\begin{aligned} \hat{\mathbf{H}}[i] &= \left(\sum_{k=1}^i \lambda^{i-k} \mathbf{r}[k] \mathbf{s}[k]^H \right) \left(\sum_{k=1}^i \lambda^{i-k} \mathbf{s}[k] \mathbf{s}[k]^H \right)^{-1} \\ &= \mathbf{D}[i] \Phi^{-1}[i] \end{aligned} \quad (25)$$

where $\Phi[i] = \sum_{k=1}^i \lambda^{i-k} \mathbf{s}[k] \mathbf{s}[k]^H$ and $\mathbf{D}[i] = \sum_{k=1}^i \lambda^{i-k} \mathbf{r}[k] \mathbf{s}[k]^H$.

To avoid the matrix inversion operation, the recursive algorithm is developed based on the matrix inversion lemma. Let us define

$$\hat{\mathbf{H}}[i] = \mathbf{D}[i] \mathbf{P}[i] \quad (26)$$

where $\mathbf{D}[i]$ can be iteratively calculated by

$$\mathbf{D}[i] = \lambda \mathbf{D}[i-1] + \mathbf{r}[i] \mathbf{s}[i]^H \quad (27)$$

and by using the matrix inversion lemma, we may calculate $P[i]$ iteratively as

$$P[i] = \lambda^{-1}P[i - 1] - \frac{\lambda^{-2}P[i - 1]s[i]s[i]^H P[i - 1]}{1 + \lambda^{-1}s[i]^H P[i - 1]s[i]} \quad (28)$$

Initially, we set the parameters $D[0] = \mathbf{0}_{N_R, N_T}$ and $P[0] = \delta_c^{-1}I$, where δ_c is a small constant.

4.3 Complexity

Here, we detail the computational complexity in terms of additions and multiplications of the proposed algorithm with the RLS implementation and other existing algorithms, namely the linear detector with RLS, the V-BLAST with RLS and the SD, as shown in Table 2. The linear detector has the lowest complexity $\mathcal{O}(N_R^2)$, and the V-BLAST has a complexity $\mathcal{O}(N^2)$, $N = \max\{N_T, N_R\}$. Our proposed algorithm has L times the complexity of the V-BLAST. Compared with the SD whose complexity is extremely high when the SNR level is low or moderate and higher modulation as well as more antennas are employed, say 16-QAM and 8×8 systems, our proposed algorithm has a fixed complexity. Note that the complexity of the SD is associated

with the constellation size M and the radius d which is chosen to be a scaled version of the noise variance [10].

In order to illustrate the main trends in what concerns the complexity of the proposed detector with the RLS algorithm and other existing algorithms, we show in Fig. 6 the complexity in terms of additions and multiplications against the number of antennas ($N_T = N_R$). In this case, our algorithm using the FSB scheme with $L = 10$ is investigated because it provides comparable performance with the SD. The curves indicate that the complexity of the SD increases sharply with the number of antennas. For a QPSK 4×4 system at the high SNR level, say 12 dB, the complexity of the SD is lower than our proposed algorithm. However, when higher modulation (16-QAM) or more antennas ($N_T, N_R \geq 6$) is employed at the moderate SNR level, for example 8 dB, the complexity of the SD is typically very high.

5 Performance analysis

In this section, a BEP performance analysis for our proposed algorithm is carried out. The BEP expression of the V-BLAST detector, rather than symbol error probability (SEP) which was discussed in [23, 24], is firstly built based on the Gaussian approximation and the MMSE criterion. It is well known that the detection with DF suffers from the

Table 2 Computational complexity of algorithms

Algorithm	Number of operations per symbol	
	Multiplications	Additions
linear MMSE-RLS	$4N_R^2 + 4N_R$	$3N_R^2 + 2N_R - 1$
V-BLAST-RLS	$4N_R^2 + 4N_T N_R + \frac{4}{3}N_T^2 - \frac{4}{3}$	$3N_R^2 + 3N_T N_R - N_R + N_T^2 - \frac{1}{2}N_T - \frac{3}{2}$
proposed-RLS	$(4N_R^2 + 4N_T N_R + \frac{4}{3}N_T^2 - \frac{4}{3})L$	$(3N_R^2 + 3N_T N_R - N_R + N_T^2 - \frac{1}{2}N_T - \frac{3}{2})L$
SD [10]	$\sum_{k=1}^{N_T} (Mk \pi^{k/2} / \Gamma(k/2 + 1))d^k + 2N_T^2$	$\sum_{k=1}^{N_T} (M(k + 1) \pi^{k/2} / \Gamma(k/2 + 1))d^k + 2N_T^2 - N_T + 2$
	Number of operations per block	
channel estimation	$N_R N_T^2 + 4N_T^2 + 2N_T N_R + 2N_T + 2$	$N_R N_T^2 + 4N_T^2 - N_T$
ordering	$N_R N_T^2 + 4N_T^2 + 2N_T N_R + 2N_T + 2$	$N_R N_T^2 + 4N_T^2 - N_T$

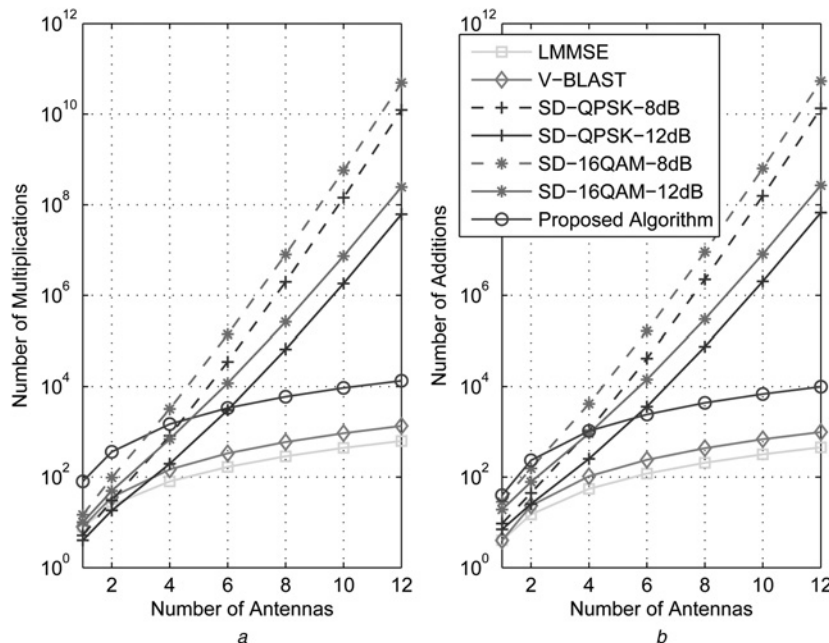


Fig. 6 Complexity in terms of arithmetic operations against number of antennas ($N_T = N_R$)

a and b $L = 10$

error propagation, that is, the cancellation of an erroneously detected symbol increases the power of the interfering terms and can cause significant performance degradation. In the following subsections, we analyse the performance of the MIMO V-BLAST receiver taking the error propagation into account. Furthermore, building on this, the BEP analysis of our proposed algorithm is carried out.

5.1 BEP performance of the V-BLAST detector

Without loss of generality, in the following, it will be assumed that in the n th step we detect the n th element $s_n[i]$ of $\mathbf{s}[i]$. It is easy to show that, with SIC, the BEP can be derived by

$$P_e = \frac{1}{N_T} \sum_{n=1}^{N_T} P_{e_n} \quad (29)$$

where P_{e_n} represents the probability of making an error in the detection of the n th symbol. Taking into account the effects of error propagation, the determination of the exact expressions for P_{e_n} is difficult. We will rely here on presenting a simple approach to estimate these probabilities. By using the total probability theorem [23], we can write

$$P_{e_n} = \sum_{j=0}^{N_n-1} \mathbb{P}\{\mathbf{e}_n | \mathbf{E}_j^{(n)}\} \mathbb{P}\{\mathbf{E}_j^{(n)}\} \quad (30)$$

where the $N_n = 2^{n-1}$ mutually exclusive error events $\mathbf{E}_j^{(n)}$, with $\mathbb{P}\left\{\bigcup_{j=0}^{N_n-1} \mathbf{E}_j^{(n)}\right\} = 1$. Each error event $\mathbf{E}_j^{(n)}$ can be associated with an $(n-1)$ -dimensional vector $\mathbf{e}_j^{(n)}$, with element $e_{j,m}^{(n)}$ equal to zero if the symbol at the m th step has been correctly detected, one otherwise. It is convenient for what follows to assume that $\mathbf{e}_j^{(n)}$ is an $(n-1)$ -dimensional vector containing the binary representation of the number j . Let us consider a simple example with $n=4$. In this case, we have $N_n=7$, and $\mathbf{e}_5^{(4)} = [1, 0, 1]^T$ represents the error event that the first and the third symbols have been incorrectly detected and the second symbol has been correctly detected. To better understand our derivation of $\mathbb{P}\{\mathbf{e}_n | \mathbf{E}_j^{(n)}\}$, we also take $n=4$ for an example. $\mathbb{P}\{\mathbf{e}_4 | \mathbf{E}_5^{(4)}\}$ represents the error probability for the fourth symbol conditioned on the error event $\mathbf{E}_5^{(4)}$. $\mathbb{P}\{\mathbf{e}_n | \mathbf{E}_j^{(n)}\}$ can be expressed by

$$\mathbb{P}\{\mathbf{e}_n | \mathbf{E}_j^{(n)}\} = Q\left(\sqrt{\gamma_{n|\mathbf{E}_j^{(n)}}}\right) \quad (31)$$

where $\gamma_{n|\mathbf{E}_j^{(n)}}$ denotes the SINR for n th detected symbol conditioned on the error event $\mathbf{E}_j^{(n)}$, and the function $Q(x)$ is defined as $Q(x) = (1/2)\text{erfc}(x/\sqrt{2})$. To derive the SINR, let us consider the received vector $\mathbf{r}_n[i]$ and the MMSE nulling vector \mathbf{W}_n according to (7) as

$$\mathbf{r}_n[i] = \sum_{l=n}^{N_T} (\mathbf{H})_l s_l[i] + \underbrace{\sum_{l=1}^{n-1} (\mathbf{H})_l (s_l[i] - \hat{s}_l[i]) + \mathbf{v}[i]}_{\tilde{\mathbf{v}}_{n|\mathbf{E}_j^{(n)}}[i]} \quad (32)$$

$$\mathbf{W}_n = \left(\bar{\mathbf{H}}_n \bar{\mathbf{H}}_n^H + \frac{\sigma_v^2}{\sigma_s^2} \mathbf{I} \right)^{-1} (\mathbf{H})_n$$

where $\tilde{\mathbf{v}}_{n|\mathbf{E}_j^{(n)}}[i]$ denotes the equivalent noise vector associated with the error event $\mathbf{E}_j^{(n)}$. It is shown that the errors in the previous symbols results in an additional disturbance, which can cause severe performance degradation. In order to approximate the model, we assume the term $\tilde{\mathbf{v}}_{n|\mathbf{E}_j^{(n)}}[i]$ to be a Gaussian r.v. with $\mathbb{E}\{\tilde{\mathbf{v}}_{n|\mathbf{E}_j^{(n)}}[i]\} = 0$ and

$$\begin{aligned} \mathbf{\Gamma}_{\tilde{\mathbf{v}}_{n|\mathbf{E}_j^{(n)}}} &= \mathbb{E}\{\tilde{\mathbf{v}}_{n|\mathbf{E}_j^{(n)}}[i] \tilde{\mathbf{v}}_{n|\mathbf{E}_j^{(n)}}[i]^H\} \\ &= \left(\sum_{l=1}^{n-1} \|(\mathbf{H})_l\|^2 \mathbb{E}\{|s_l[i] - \hat{s}_l[i]|^2\} + \frac{\sigma_v^2}{\sigma_s^2} \right) \mathbf{I} \end{aligned} \quad (33)$$

Thus, the desired signal covariance matrix and the interference-plus-noise covariance matrix for the n th detection can be written as $\mathbf{R}_s^n = \sigma_s^2 (\mathbf{H})_n (\mathbf{H})_n^H$ and $\mathbf{R}_{i,n|\mathbf{E}_j^{(n)}} = \bar{\mathbf{H}}_n \bar{\mathbf{H}}_n^H + \mathbf{\Gamma}_{\tilde{\mathbf{v}}_{n|\mathbf{E}_j^{(n)}}}$, respectively. Actually, the interference-plus-noise covariance matrix is associated with the error event and the equivalent noise power caused by error propagation is increased. Therefore the output SINR of the n th detected symbol conditioned on the error event $\mathbf{E}_j^{(n)}$ can be given as

$$\gamma_{n|\mathbf{E}_j^{(n)}} = \frac{\mathbf{W}_n^H \mathbf{R}_s^n \mathbf{W}_n}{\mathbf{W}_n^H \mathbf{R}_{i,n|\mathbf{E}_j^{(n)}} \mathbf{W}_n} \quad (34)$$

Substituting (34) into (31), we can obtain the conditioned error probability $\mathbb{P}\{\mathbf{e}_n | \mathbf{E}_j^{(n)}\}$. Now consider the evaluation of $\mathbb{P}\{\mathbf{E}_j^{(n)}\}$, which can be written as

$$\mathbb{P}\{\mathbf{E}_j^{(n)}\} = \mathbb{P}\{\mathbf{e}_j^{(n)}\} = \mathbb{P}\{\cap_{m=1}^{n-1} e_{j,m}^{(n)}\} \quad (35)$$

By using the well-known property of conditional probability $\mathbb{P}\{\cap_{m=1}^N A_m\} = \prod_{m=1}^N \mathbb{P}\{A_n | \cap_{k=1}^{m-1} A_k\}$, we obtain

$$\begin{aligned} \mathbb{P}\{\cap_{m=1}^{n-1} e_{j,m}^{(n)}\} &= \prod_{m=1}^{n-1} \mathbb{P}\{e_{j,m}^{(n)} | \cap_{k=1}^{m-1} e_{j,k}^{(n)}\} \\ &= \mathbb{P}\{e_{j,n-1}^{(n)} | \cap_{k=1}^{n-2} e_{j,k}^{(n)}\} \\ &\quad \times \mathbb{P}\{e_{j,n-2}^{(n)} | \cap_{k=1}^{n-3} e_{j,k}^{(n)}\} \dots \mathbb{P}\{e_{j,1}^{(n)}\} \end{aligned} \quad (36)$$

where the term $\mathbb{P}\{e_{j,n-1}^{(n)} | \cap_{k=1}^{n-2} e_{j,k}^{(n)}\}$ represents the probability of an error decision $e_{j,n-1}^{(n)} = 1$ or a correct decision $e_{j,n-1}^{(n)} = 0$ when detecting the $(n-1)$ th symbol conditioned on the detection if the first $(n-2)$ symbols. By substituting (31) and (36) into (30) and then substituting (30) into (29), we finally can calculate the average BEP P_e as

$$\begin{aligned} P_e &= \frac{1}{N_T} \sum_{n=1}^{N_T} \sum_{j=0}^{N_n-1} Q\left(\sqrt{\gamma_{n|\mathbf{E}_j^{(n)}}}\right) \\ &\quad \times \mathbb{P}\{e_{j,n-1}^{(n)} | \cap_{k=1}^{n-2} e_{j,k}^{(n)}\} \\ &\quad \times \mathbb{P}\{e_{j,n-2}^{(n)} | \cap_{k=1}^{n-3} e_{j,k}^{(n)}\} \dots \mathbb{P}\{e_{j,1}^{(n)}\} \end{aligned} \quad (37)$$

It is worth noting that because the binary digits in the error event vector represent the symbol error, the BEPs calculated in (35) have to be converted from SEPs unless the modulation scheme is binary phase-shift keying.

5.2 BEP performance of the MB-SIC detector

Based on the above analysis, the simplest method is to extend the analysis straightforwardly to our proposed MB-SIC detector. By using (29) to calculate the BEPs $\{P_e^{(l)}|l = 1, \dots, L\}$ for all branches, we may select the branch with the minimum error probability as the optimum one, which is expressed as

$$l_{\text{opt}} = \arg \min_{1 \leq l \leq L} P_e^{(l)} \quad (38)$$

However, this straight method does not outline the performance of the proposed MB-SIC detector as we expected because the error probability $P_e^{(l)}$ in (38) is a statistical average value of the bit error calculated by $Q(\cdot)$, while the proposed MB-SIC detector selects the best estimates according to the selection rules at every time instant. Thus we have to build a further model to describe the performance of the proposed detector (at least a lower bound).

In this paper, we provide an approximate method to outline the lower bound for the MB-SIC scheme. Based on (37), we know that the BEP for each branch is an average of error probabilities of N_T substreams, which are calculated by conditioning on the error events associated with previous detected symbols. Now we extend the analysis in the previous section from single branch to multiple branches in an approximate way to provide an error bound. Let us consider an extreme case that the MB structure is smart enough to select the branch with the minimal BEP at every transmit substream. That is, the error probabilities selected are the minimum for detecting any symbol at any cancellation stage. The lower bound, which we define as MB lower bound (MBLB), can be written mathematically as

$$P_e = \frac{1}{N_T} \sum_{n=1}^{N_T} P_{e_n}^{(l'_{\text{opt},n})}, \quad l'_{\text{opt},n} = \arg \min_{1 \leq l \leq L} P_{e_n}^{(l)} \quad (39)$$

where $l'_{\text{opt},n}$ is the index of the branch with minimal error probability for detecting the n th symbol, $P_{e_n}^{(l)}$ denotes the error probability for detecting the n th symbol in the l th branch, which can be calculated by using (30) with the l th ordering pattern. Note that as we mentioned in the previous section, MBLB is also sensitive to the employed ordering scheme.

6 Simulations

In this section, we assess the bit error rate (BER) performance of the proposed scheme and the existing MIMO detection schemes, namely, the ML detector, the linear MMSE detector, the V-BLAST, the PIC and the proposed MB-SIC algorithm. Here, we consider two channel models in the simulation: the first one is i.i.d. random fading, whose coefficients are taken from complex Gaussian random variables with zero mean and unit variance, and the second one is the 3 GPP spatial model (SCM) [25], which was developed as a common reference for evaluating different MIMO concepts in outdoor environments at a centre frequency of 2 GHz and a system bandwidth of 5 MHz. We define the SNR as $\text{SNR} = 10 \log_{10}(N_T \sigma_s^2 / \sigma^2)$, where σ_s^2 is the variance of the transmitted symbols and σ^2 is the noise variance. In all experiments, the blocking fading channel model is assumed.

6.1 Non-adaptive detector

In these experiments, we average the experiments over 5000 runs and use packets with 100 symbols per stream employing QPSK modulation. We first compare the BER performance against SNR for our proposed detector by employing the three candidate selection rules. As shown in Fig. 7, the detector with the ML criterion outperforms the other criteria while the channel information is known. The selection rule can be chosen according to the different application requirements. In our following simulations for the non-adaptive detector, the ML criterion is the selection rule because we assume that the channel information is perfectly known.

Let us consider the proposed MB-SIC detector and the existing algorithms in the i.i.d. random flat-fading model. In Fig. 8, we evaluate the BER performance against SNR for MIMO systems with $N_T = N_R = 4$ antennas. We compare the proposed ordering algorithms with the optimal ordering scheme described in the previous section. We also compare the proposed MB-SIC detectors with different ordering schemes against the existing linear MMSE detector, V-BLAST, MMSE-PIC and ML detector. For our proposed

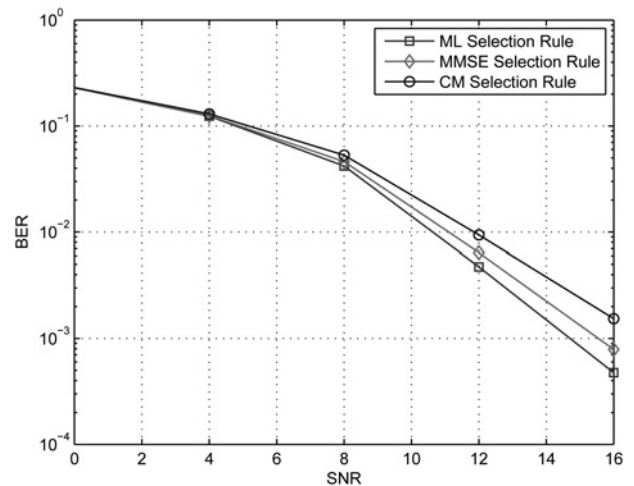


Fig. 7 BER against SNR performance comparison between the candidate selection rules for our proposed detector ($N_T = N_R = 4$)

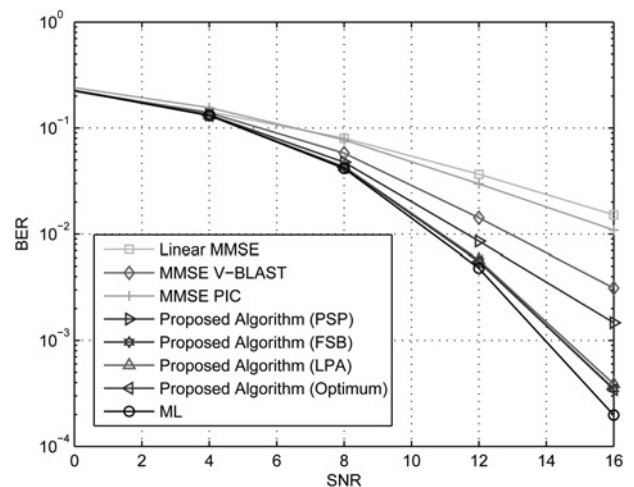


Fig. 8 BER against SNR performance comparison between the proposed algorithm and the existing algorithms for MIMO spatial multiplexing with QPSK and $N_T = N_R = 4$

ordering schemes, we have to configure the number of branches L . In this context, the maximum L is set to N_T for the PSP scheme because of the algorithm limitation. For the FSB and the LPA schemes, we set $L = 10$ considering the tradeoff between computational complexity and the performance. The performance of the proposed MB-SIC detectors outperforms the linear MMSE, the V-BLAST and the MMSE-PIC detectors. The plots also show that the performance of the proposed detector with optimal ordering scheme, which tests all $N_T!$ possible branches and selects the most likely estimate, approaches the optimal ML detector closely and the proposed detector with the FSB and the LPA schemes performs as well as that with optimal ordering.

As depicted in Fig. 9, the BER performance against SNR is investigated when the MIMO system with $N_T = N_R = 4$ antennas is working in the 3 GPP SCM environment. We use the MATLAB implementation of SCM developed by Salo *et al.* [26]. The plots show a similar result as in Fig. 8. The performance of the proposed detector with the optimal ordering scheme approaches the optimal ML detector, and the FSB scheme is slightly better than the LPA scheme.

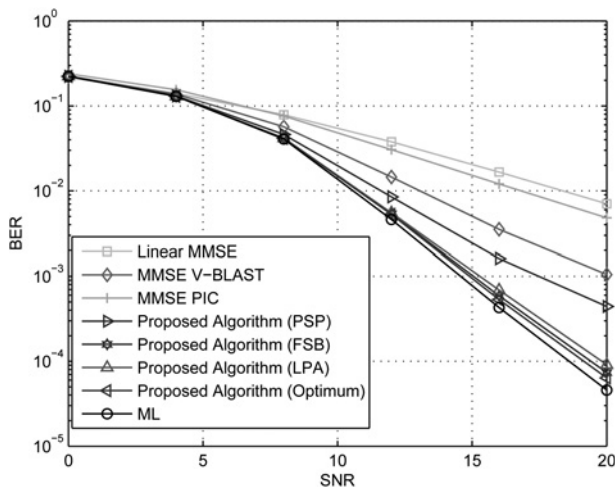


Fig. 9 BER against SNR performance comparison between the proposed algorithm and the existing algorithms for MIMO spatial multiplexing using SCM with QPSK and $N_T = N_R = 4$

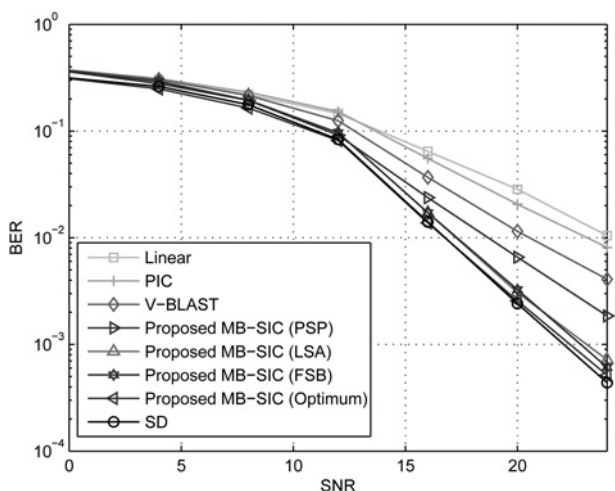


Fig. 10 BER against SNR performance comparison between the proposed algorithm and the existing algorithms for MIMO spatial multiplexing with 16-QAM and $N_T = N_R = 4$

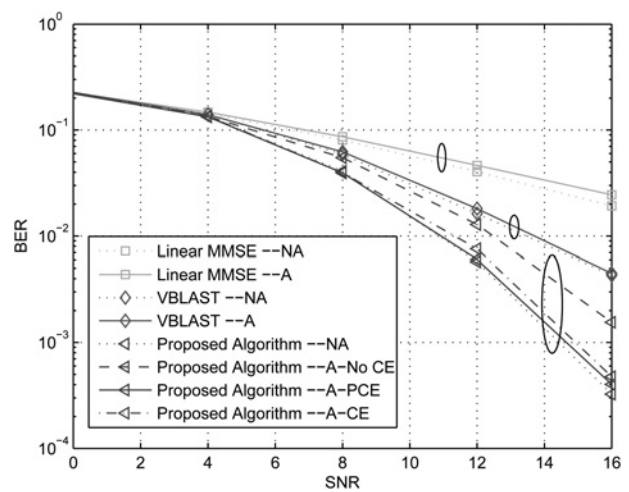


Fig. 11 BER against SNR performance for adaptive implementations of the proposed algorithm and the existing algorithms for MIMO spatial multiplexing, where A and NA denote adaptive and non-adaptive, respectively, and CE and PCE denote channel estimation and perfect channel estimation, respectively. $N_T = N_R = 4$, $\lambda = 0.998$

In Fig. 10, the BER performance against SNR is investigated when the MIMO system here $N_T = N_R = 4$ antennas and 16-QAM. The plots show that the performance of the proposed detector with the optimal ordering scheme approaches the SD scheme, and the FSB scheme is slightly better than the LPA scheme. Note that our proposed scheme has lower complexity at the lower and moderate SNR level, which would benefit coded system to some extent.

6.2 Adaptive detector

Fig. 11 shows the BER against SNR performance of the proposed detector using an adaptive implementation based on the RLS algorithm. In this experiment, we employ 50 training symbols and 500 information symbols per stream in one packet and the results are averaged over 5000 runs. The forgetting factor λ is 0.998. It is shown that the performance of the adaptive receivers with perfect channel estimation matches that of their non-adaptive counterparts

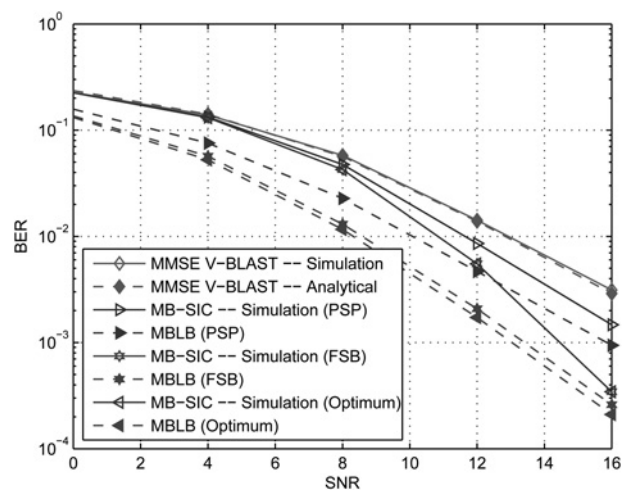


Fig. 12 BER performance comparison between the simulation results and the analytical results for both MMSE-VBLAST and our proposed MB-SIC algorithm ($N_T = N_R = 4$)

with much lower complexity. We also can find that the proposed algorithm with LS channel estimation is slightly worse than perfect channel estimation, outperforming the proposed algorithm without channel estimation and V-BLAST receiver.

6.3 Analytical results

The BER performance comparison between the simulation results and the analytical results is shown in Fig. 12. We investigate the MMSE V-BLAST algorithm, the MB-SIC algorithms with PSP, FSB and the optimum ordering schemes in the MIMO system with $N_T = N_R = 4$. The plots depict that the analytical BER performance of the MMSE V-BLAST algorithm is a perfect match with the simulation result and MBLBs with the ordering schemes bound the performance of MB-SIC with the corresponding ordering schemes, respectively. Although there are gaps between the simulation results and MBLB because of the approximate method we employ, it makes sense that the MBLB is highly related with the ordering scheme. Comparing the MBLBs, we can find that the FSB, which has ten branches, performs significantly better than the four-branch PSP scheme and slightly worse than the optimum ordering scheme which has 24 branches, which matches the simulation results.

7 Conclusions

We presented a novel MMSE SIC detector based on multiple parallel branches for a MIMO spatial multiplexing system. The proposed detection structure is equipped with SICs on several parallel branches which employ different ordering patterns. Namely, each branch produces a symbol estimate vector by exploiting a certain ordering pattern. Thus, there is a group of symbol estimate vectors at the end of the MB structure. Based on different application requirements, different criteria, such as ML, MMSE and CM, can be used as selection rules to select the branch with the best performance. We also proposed three sub-optimal ordering schemes together with the optimal ordering scheme. Furthermore, we developed an adaptive implementation for our proposed MB-SIC receiver with channel estimation based on the RLS algorithm. The proposed MMSE-MB-SIC detector, which achieves higher detection diversity, was compared with several existing detectors in the literature via computer simulations and was shown to approach the optimal ML detector while reducing the complexity significantly.

8 References

- Gans, M.J., Foschini, G.J.: 'On limits of wireless communications in a fading environment when using multiple antennas', *Wirel. Pers. Commun.*, 1998, **6**, pp. 311–335
- Telatar, I.E.: 'Capacity of multi-antenna Gaussian channels', *Eur. Trans. Telecommun.*, 1999, **10**, (6), pp. 585–595
- Foschini, G.J.: 'Layered space-time architecture for wireless communication in a fading environment when using multiple antennas', *Bell Lab. Tech. J.*, 1996, **1**, (2), pp. 41–59
- Golden, G.D., Foschini, C.J., Valenzuela, R.A., Wolniansky, P.W.: 'Detection algorithm and initial laboratory results using V-BLAST space-time communication architecture', *Elect. Lett.*, 1999, **35**, (1), pp. 14–16
- Wolniansky, P.W., Foschini, G.J., Golden, G.D., Valenzuela, R.A.: 'V-BLAST: an architecture for realizing very high data rates over the rich-scattering wireless channel'. URSI Int. Symp. on Sig., Sys., and Elec., 1998, ISSSE 98, 29 September–2 October, 1998
- Alamouti, S.: 'A simple transmit diversity technique for wireless communications', *IEEE J. Sel. Areas Commun.*, 1998, **16**, (8), pp. 1451–1458
- Tarokh, V., Jafarkhani, H., Calderbank, A.R.: 'Space-time block codes from orthogonal designs', *IEEE Trans. Inf. Theory*, 1999, **45**, pp. 1456–1467
- Verdu, S.: 'Multiuser detection' (Cambridge Univ. Press, Cambridge, UK, 1998)
- Viterbo, E., Boutros, J.: 'A universal lattice code decoder for fading channels', *IEEE Trans. Inf. Theory*, 1999, **45**, (5), pp. 1639–1642
- Hassibi, B., Vikalo, H.: 'On the sphere decoding algorithm: part I, the expected complexity', *IEEE Trans. Signal Process.*, 2005, **53**, (8), pp. 2806–2818
- Patel, P., Holtzman, J.: 'Analysis of a simple successive interference cancellation scheme in a DS/CDMA systems', *IEEE J. Sel. Areas Commun.*, 1994, **12**, (5), pp. 796–807
- Duel-Hallen, A.: 'Equalizers for multiple input multiple output channels and PAM systems with cyclostationary input sequences', *IEEE J. Sel. Areas Commun.*, 1992, **10**, pp. 630–639
- Al-Dhahir, N., Sayed, A.H.: 'The finite-length multi-input multi-output MMSK-DFK', *IEEE Trans. Signal Process.*, 2000, **48**, (10), pp. 2921–2936
- de Lamare, R.C., Sampaio-Neto, R.: 'Adaptive MBER decision feedback multiuser receivers in frequency selective fading channels', *IEEE Commun. Lett.*, 2003, **7**, (2), pp. 73–75
- de Lamare, R.C., Sampaio-Neto, R.: 'Minimum mean-squared error iterative successive parallel arbitrated decision feedback detectors for DS-CDMA systems', *IEEE Trans. Commun.*, 2008, **56**, (5), pp. 778–789
- Varanasi, M.K., Aazhang, B.: 'Multistage detection in asynchronous CDMA communications', *IEEE Trans. Commun.*, 1990, **38**, (4), pp. 509–519
- de Lamare, R.C., Sampaio-Neto, R., Hjørungnes, A.: 'Joint iterative interference cancellation and parameter estimation for CDMA systems', *IEEE Comm. Lett.*, 2007, **11**, (12), pp. 916–918
- Choi, J.H., Yu, H.Y., Lee, Y.H.: 'Adaptive MIMO decision feedback equalization for receivers with time-varying channels', *IEEE Trans. Signal Process.*, 2005, **53**, (11), pp. 4295–4303
- Ginis, G., Cioffi, J.M.: 'On the relation between V-BLAST and the GDFE', *IEEE Commun. Lett.*, 2001, **5**, (9), pp. 364–366
- Godard, D.: 'Self-recovering equalization and carrier tracking in two-dimensional data communication systems', *IEEE Trans. Commun.*, 1980, **28**, (11), pp. 1867–1875
- Thaiupatump, T., Kassam, S.A.: 'Square contour algorithm: a new algorithm for blind equalization and carrier phase recovery'. Proc. 37th Asilomar Conf. on Signals, Systems and Computers, 2003, pp. 647–751
- Karami, E.: 'Tracking performance of least squares MIMO channel estimation algorithm', *IEEE Trans. Commun.*, 2007, **55**, (11), pp. 2201–2209
- Chiani, M., Win, M.Z., Zanella, A., Winters, J.H.: 'Bounds and approximations for optimum combining of signals in the presence of multiple co-channel interferers and thermal noise', *IEEE Trans. Commun.*, 2003, **51**, (2), pp. 296–307
- Zanella, A., Chiani, M., Win, M.Z.: 'MMSE reception and successive interference cancellation for MIMO systems with high spectral efficiency', *IEEE Trans. Wirel. Commun.*, 2005, **4**, (3), pp. 296–307
- 3GPP: 'Spatial channel model for multiple input multiple output (MIMO) simulations'. 3GPP, TR 25.996, v6.1.0. Available at: www.3gpp.org
- Salo, J., Galdo, G.D., Kyosti, P., Milojevic, M., Laselva, D., Schneider, C.: 'MATLAB implementation of the 3 GPP spatial channel model (3 GPP TR 25.996)', January 2005, On-line: <http://www.tkk.fi/units/radio/scm/>